JOURNAL OF NATURAL PRODUCTS

ARTICLE

pubs.acs.org/jnp

Diversonol and Blennolide Derivatives from the Endophytic Fungus *Microdiplodia* sp.: Absolute Configuration of Diversonol

Imran Nafees Siddiqui,[†] Aqib Zahoor,[†] Hidayat Hussain,[†] Ishtiaq Ahmed,[†] Viqar Uddin Ahmad,[‡] Daniele Padula,[§] Siegfried Draeger,[⊥] Barbara Schulz,[⊥] Kathrin Meier,[⊥] Michael Steinert,[⊥] Tibor Kurtán,[∥] Ulrich Flörke,[†] Gennaro Pescitelli,*[,§] and Karsten Krohn*[,†]

[†]Department of Chemistry, University of Paderborn, Warburger Strasse 100, 33098-Paderborn, Germany

[‡]HEJ Research Institute of Chemistry, International Centre for Chemical and Biological Sciences, University of Karachi, Karachi-75270, Pakistan

[§]Department of Chemistry, University of Pisa, Via Risorgimento 35, I-56126 Pisa, Italy

[⊥]Institute of Microbiology, Technical University of Braunschweig, Spielmannstrasse 7, 31806 Braunschweig, Germany

[∥]Department of Organic Chemistry, University of Debrecen, PO Box 20, H-4010 Debrecen, Hungary

Supporting Information

ABSTRACT: Chemical investigation of the fungal strain *Microdiplodia* sp. isolated from the shrub *Lycium intricatum* led to the isolation of four new compounds: a hexahydroxanthone (**2**), a 2,3-dihydrochroman-4-one (**3**), a 7-oxoxanthone derivative (**4**), and a 1,4-oxazepan-7-one (**5**). The relative configurations of the new compounds were determined by intensive NMR investigations, notably NOESY experiments at different temperatures. The absolute configurations of the well-known fungal metabolite diversonol (**1**) and of other xanthone derivatives (**3**, **4**) were established by means of TDDFT ECD calculations. Most of the metabolites were biologically active, with antibacterial activity against *Legionella pneumophila* and/or antifungal activity against *Microbotryum violaceum*.

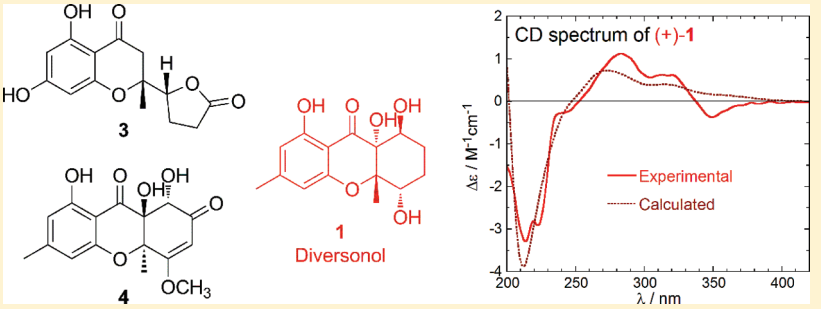

Endophytic fungi have been proven to be a rich source of new biologically active natural products because as a group they inhabit a relatively untapped ecological environment, and their secondary metabolism is activated by their metabolic interactions with their hosts.[1] Xanthones and partially hydrogenated di- or tetrahydroxanthones are widespread classes of natural products[2] with considerable bioactivity that occur in fungi,[3] plants,[4] ferns,[5] and lichens.[6] Owing to their pronounced toxicity, they are classified as mycotoxins.[3] The tetrahydroxanthones occur as monomers, for example, as α- and β-diversonolic esters, monodictysins, or blennolides, the recently isolated monomeric units of secalonic acids.[7] Other examples of highly active anticancer hydrogenated xanthones are globosuxanthone A,[8] nidulalin A,[9] xanthoquinodins,[10] and parnafungins.[11] Fungal secondary metabolites have served as an important source of lead structures for new drug compounds.[11,12] In our screening program for new biologically active fungal secondary metabolites we have been investigating the metabolites of fungal endophytes, presently of an endophytic *Microdiplodia* sp. The EtOAc extract was subjected to column chromatography, and four new metabolites (**2**−**5**) were isolated, together with six known compounds (**1**, **6**−**10**). The new compounds were named microdiplodiasol (**2**), microdiplodiasone (**3**), microdiplodiasolol (**4**), and microdiplactone (**5**).

RESULTS AND DISCUSSION

The endophytic fungus *Microdiplodia* sp. (internal strain no. 9907) was isolated from the shrub *Lycium intricatum*, from Gomera, and cultivated at room temperature on biomalt solid agar media for 28 days. The culture media (12 L) were then extracted with EtOAc to afford a crude extract (5.5 g), and in order to perform an efficient targeted isolation of active metabolites, the EtOAc extract was subjected to column chromatography, resulting in the isolation of 10 metabolites (**1**−**10**) (Scheme 1).

The structure of diversonol (**1**), the major metabolite of the title fungus, was determined by detailed spectroscopic analysis

Special Issue: Special Issue in Honor of Koji Nakanishi

Received: October 19, 2010
Published: January 18, 2011

Scheme 1. Structures of Compounds 1−10 Isolated from *Microdiplodia* sp.

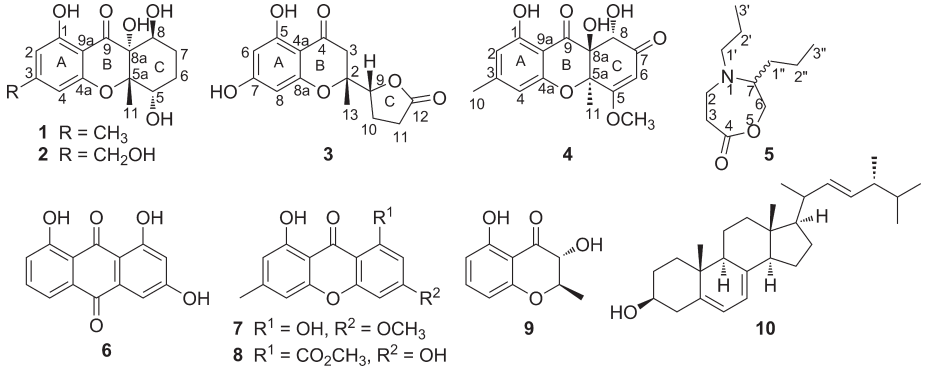

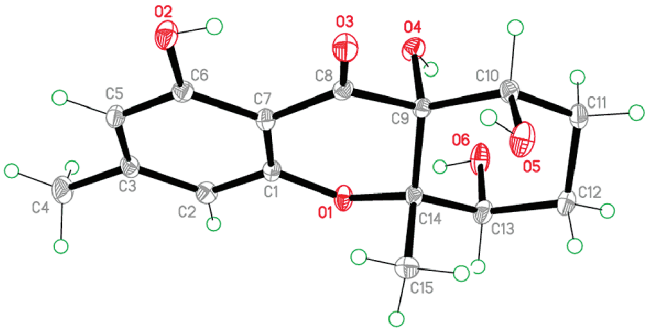

Figure 1. Molecular structure of **1**. Displacement ellipsoids are drawn at the 50% probability level. Labels are related to the deposited cif file (see Experimental Section) and do not correspond to the numbering shown in Scheme 1.

and comparison with reported data.[13,14] The absolute configuration of this well-known compound is not known.[13,15] Therefore, we elucidated the absolute configuration of diversonol (**1**), as well as of the new compounds **3** and **4**, by comparing their electronic CD spectra (ECD) with those calculated by the time-dependent DFT method (TDDFT).[16,17] Since diversonol (**1**) was obtained in crystalline form suitable for X-ray analysis (Figure 1), we first thought to employ our solid-state ECD/TDDFT approach[17] to determine its absolute configuration.

For this purpose, ECD spectra of (+)-**1** were recorded in MeOH solution and in the microcrystalline solid state as a KCl pellet (Figure 2a). However, the two spectra were not as similar as it would be expected on the basis of the apparently rigid molecular structure of **1**. The differences are especially evident in the region around the absorption maximum at 282 nm (ε = 2800 M^{-1} cm^{-1} in MeOH) due to the ^1L_a-type transition of the aromatic chromophore. It is likely that between 260 and 330 nm the solid-state ECD spectrum is affected by intermolecular exciton couplings between molecules closely packed in the crystals.[17] This situation is not ideal for application of the solid-state ECD/TDDFT approach, which relies on single-molecule calculations. Therefore, we focused on the solution ECD spectrum of compound **1**; the same choice was more obvious for compounds **3** and **4**, whose X-ray structures were not available. The ECD spectra of the three compounds, belonging to the family of chromanones, are almost entirely determined by the helicity assumed by ring B (see Scheme 1), which is in turn dictated by the substituents on the same ring.[18] For compound **1**, the configuration of the stereogenic centers C-5a and C-8a is the major determinant of the observed ECD spectrum, and for an assumed (5a*S*,8a*R*) absolute configuration ring B acquires a so-called *M* helicity (negative C-4a−O−C-5a−C-8a dihedral angle).

Following a standard procedure for the prediction of solution ECD spectra,[16,17] the conformational ensemble of **1** in solution was investigated by a molecular mechanics conformational search (using the MMFF force field) followed by DFT geometry optimizations at the B3LYP/6-31G(d) level, using input structures with a (5*S*,5a*S*,8*S*,8a*R*) configuration. To obtain more reliable structures and free energies, DFT geometry optimizations and frequency calculations were run at the B3LYP/6-311+G(d,p) level including the PCM solvation model for MeOH. This procedure afforded for **1** three energy minima with free energies within 2.5 kcal/mol (see Supporting Information), which differed only in the orientation of some OH groups. In particular, the most stable conformer (55% Boltzmann population at 300 K; see structure in the Supporting Information) is similar to the X-ray structure shown in Figure 1. This finding supports the assumption that the difference between solution and solid-state ECD spectra of **1** is not related to a different conformation. After screening of several combinations of functionals and basis sets (see Computational Section and Supporting Information), ECD spectra were calculated for the three low-energy DFT structures with TDDFT at the B3LYP/aug-TZVP level, including PCM for MeOH, and averaged using respective Boltzmann populations (estimated from free energies) at 300 K (Figure 2b). The agreement between the experimental and calculated spectra in MeOH is very good in the wavelength region below 330 nm. At long wavelengths, the negative experimental ECD Cotton effect at 360 nm is missing in the calculated spectrum. Actually, a small positive rotational strength is predicted for the first transition calculated at 355−365 nm, which is mainly of $\pi-\pi^*$ character (aromatic ^1L_b band). It must be stressed that this kind of band is often problematic for TDDFT calculations.[19] This minor discrepancy does, however, not preclude the assignment of the absolute configuration of diversonol (+)-(**1**) as 5*S*,5a*S*,8*S*,8a*R*. To further substantiate the result, we calculated optical rotations[20] at the D line for the three low-energy structures with a (5*S*,5a*S*,8*S*,8a*R*) configuration at the same B3LYP/aug-TZVP level. The three values were all positive and in the range between +86 and +118, their weighted average was +87.6, in agreement with the experimental value of $[\alpha]_D$ +70 ± 2.

Microdiplodiasol (**2**) was obtained as an optically active, brown gum. The molecular formula $C_{15}H_{18}O_7$, indicating seven

dx.doi.org/10.1021/np100730b |*J. Nat. Prod.* 2011, 74, 365–373

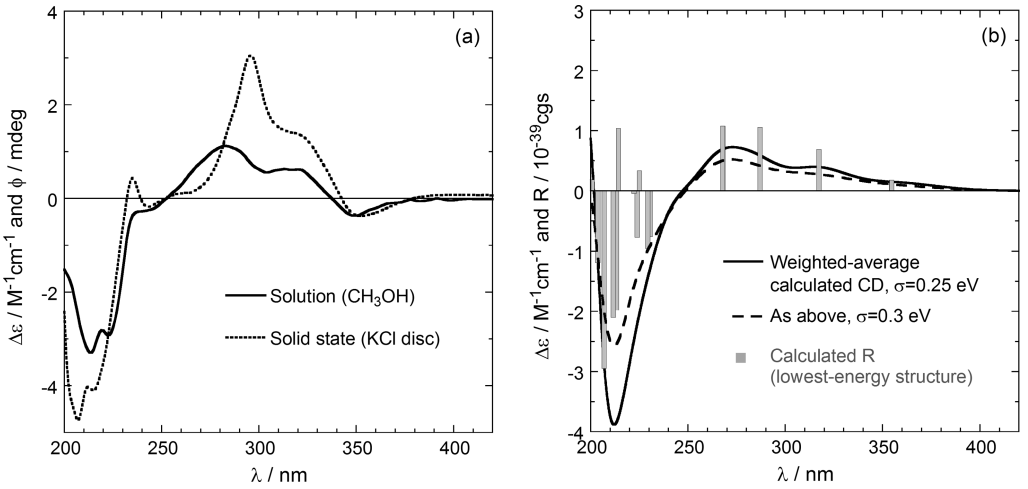

Figure 2. ECD spectra of (5*S*,5a*S*,8*S*,8a*R*)-(+)-diversonol (**1**). (a) Experimental spectra in MeOH solution and in the solid state (as KCl disk, expressed in ellipticity ϕ). (b) Weighted-average TDDFT-calculated spectrum at B3LYP-SCRF/aug-TZVP//B3LYP-SCRF/6-311+(d,p) level with PCM in MeOH. Vertical bars represent rotational strengths calculated for the lowest-energy conformer; σ is the applied Gaussian band shape.

Scheme 2. COSY and Key HMBC Correlations for Compound 2

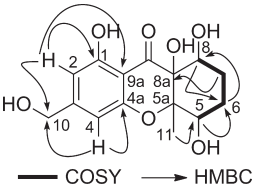

double-bond equivalents, was established by HREIMS. The IR spectrum of **2** showed the presence of hydroxy groups (3245 cm^{-1}), a carbonyl functionality (1649 cm^{-1}), and a typical 1,2,3-trisubstituted aromatic system (1633, 1572, 716 cm^{-1}). These observations were in agreement with the observation of signals in the ^{13}C NMR and DEPT spectra (see Experimental Section) for two secondary oxygenated carbons [δ_C 69.7 (C-8), 66.9 (C-5)], a conjugated ketone carbonyl atom (δ_C 194.4, s), and six aromatic carbons (δ_C 162.1, s; 158.5, s; 153.2, s; 105.9, d; 105.7, d; 104.6, s) accounting for five double-bond equivalents. The remaining double-bond equivalents were due to the presence of two further rings. The ^1H NMR data of **2** revealed the presence of two hydrogen-bonded hydroxy groups at δ_H 12.31 (1H, s) and 11.30 (1H, s), one (δ_H 12.31) of which had to be placed at C-1 and the second one (δ_H 11.30) at C-8a. The absence of aromatic signals around δ_H 7.40−7.60 in the ^1H NMR spectrum was consistent with the lack of protons *peri* to the carbonyl group.[6] The ^1H NMR spectrum also showed two aromatic protons at δ_H 6.51 and 6.62 in a *m*-arrangement and one methyl singlet at δ_H 1.56. The positions of the former groups were further established according to HMBC correlations of H-2 with C-3, C-4, and C-9a and of H-4 with C-4a, C-2, and C-9a (Scheme 2). The structure of **2** was determined by comparison of its spectroscopic data with those of **1**.[13] The molecular ion peak of compound **2**, which is 16 amu higher than compound **1**, indicated the presence of one extra oxygen atom. Other differences were apparent in the ^1H and ^{13}C NMR spectra. Two methylene protons [δ_H 4.59 (2H, d, J = 5.5 Hz)] appeared in the ^1H NMR spectrum of **2** instead of a three-proton signal for an aromatic methyl at C-3 [δ_H 2.24 (3H, s)] as found in compound **1**. Similarly, the ^{13}C NMR spectrum showed the disappearance of the methyl carbon atom [δ_C 21.9 (C-10) in **1**], which was replaced by a methylene carbon atom (δ_C 63.5) at C-3. The structure of **2** was unequivocally determined by 2D NMR experiments, which gave corresponding COSY and HMBC correlations (Scheme 2).

Compound **3** was obtained as a yellow gum, whose molecular formula $C_{14}H_{14}O_6$ was determined by HREIMS. The UV spectrum showed bands at 211, 278, and 348 nm, while the IR spectrum displayed bands at 3384, 1776, and 1642 cm^{-1} characteristic for hydroxy, γ-lactone carbonyl, and conjugated ketone carbonyl groups, respectively. The ^{13}C NMR spectrum (see Experimental Section) showed resonances at δ_C 176.6 and 196.6, supporting the presence of γ-lactone and ketone carbonyl groups. The ^1H NMR spectrum exhibited resonances for one hydrogen-bonded hydroxy group (δ_H 11.57, s), two aromatic protons (δ_H 7.11, br s, and 7.21, br s), one oxymethine proton (δ_H 4.58, t, J = 7.2 Hz), three methylene groups [δ_H 2.98 (d, J = 17.1 Hz, 1H), 2.61 (d, J = 17.1 Hz, 1H), 2.60 (m, 2H), and 2.32 (m, 2H)], and one oxyquaternary methyl group (δ_H 1.43, s). HMBC and NOEDIFF results indicated that **3** possessed an aromatic ring A identical to **1**, except that the aromatic methyl group at C-3 was missing in the ^1H and ^{13}C NMR spectra and was replaced by a hydroxy group in compound **3**. The nonequivalent methylene protons at δ_H 2.98 and 2.61 were attributed to H_2-3 of the chromanone skeleton due to their correlations with C-2 (δ_C 81.1), C-4 (δ_C 196.6), and C-13 (δ_C 18.8) in the HMBC spectrum. The oxyquaternary methyl group resonating at δ_H 1.43 gave a HMQC cross-peak with C-13 and HMBC correlations (Scheme 3) from the methyl protons to C-2 and C-3 (δ_C 42.8). In the COSY spectrum, the methylene protons at δ_H 2.32 (H_2-10) were coupled with the methylene protons at δ_H 2.60 (H_2-11) and the oxymethine proton at δ_H 4.58 (H-9). These results together with a ^3J HMBC cross-peak from H-9 to the carbonyl carbon at δ_C 176.6 (C-12) confirmed the presence of the γ-lactone moiety. Bond formation between C-9 of the γ-lactone unit and C-2 of the chromanone skeleton was established on the basis of ^3J HMBC correlations of H-9 with C-3 and C-13. The NOEDIFF results between H-9 and H_3-13 and H-3α

dx.doi.org/10.1021/np100730b |*J. Nat. Prod.* 2011, 74, 365–373

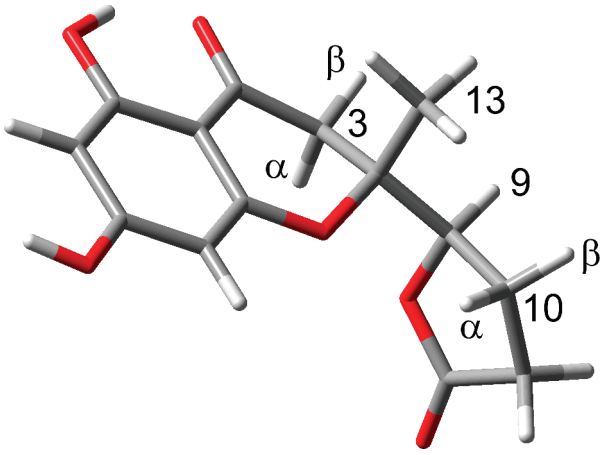

Figure 3. Structure of the absolute lowest-energy conformer of (2*R*,9*R*)-(+)-microdiplodiasone (**3**) calculated at the B3LYP-SCRF/6-311+(d,p) level with PCM in MeOH.

(2.98, d, J = 17.1 Hz) and those between H_3-13 and H-9 and H-3β (δ 2.61, d, J = 17.1 Hz) revealed that both H-9 and H_3-13 have a β-orientation. The structure of microdiplodiasone (**3**) was determined as 5,7-dihydroxy-2-methyl-2-(5-oxotetrahydro-2-furanyl)-2,3-dihydro-4*H*-chromen-4-one. The structure of chromanone **3** closely resembles that of lachnone C,[21] with the only difference being the presence of a hydroxy rather than a hydroxymethyl substituent at C-7. Its structure is also similar to the recently isolated blennolides D−F,[7] albeit with differences including the presence of a hydroxy group at C-7, the absence of substituents at C-10 and C-11, and the replacement of a methoxycarbonyl with a C-13 methyl group.

Additional NOESY experiments were done in acetonitrile-d_3 for better comparison with ECD spectra measured in the same solvent, and the principal results are displayed in Scheme 3. The strong NOE between CH_3-13 and H-3β and the absence of a corresponding NOE between CH_3-13 and H-3α revealed that the 13-methyl group occupies a preferential axial position relative to ring B; the lactone ring is equatorially oriented. Very importantly, only a weak NOE association was observed between H-3α and H-10α, which, however, disappeared at −20 °C (while the remaining NOE network was almost unchanged). These findings were useful to assign the relative configuration at the two stereogenic centers when rationalized with the help of molecular modeling. Two diastereomeric starting structures with (2*R*,9*R*) and (2*R*,9*S*) configuration were subjected to the same modeling protocol described for compound **1**. However, microdiplodiasone (**3**) is conformationally more flexible, so several low-energy minima were obtained for the two diastereomers, that is, 10 and 12 structures with DFT free energies within 1.6 kcal/mol for (2*R*,9*R*)-**3** and (2*R*,9*S*)-**3**, respectively (calculated at the B3LYP-SCRF/6-311+G(d,p) level with PCM in acetonitrile; see Supporting Information). The most important degree of conformational freedom is the conformation assumed by ring B, which, as explained above, determines the shape of the ECD spectrum. For both diastereomers, structures with an axial 13-methyl group were favored over those with an equatorial 13-methyl group; that is, the lactone groups showed a stronger preference for the equatorial position. Structures with an axial 13-methyl group accounted for 77% overall population at 300 K for (2*R*,9*R*)-**3** and 85% for (2*R*,9*S*)-**3**, respectively. The most important difference between the two conformational ensembles lies in the

Scheme 3. COSY and Key HMBC Correlations (top) and Relevant NOEs (bottom) for Compound 3

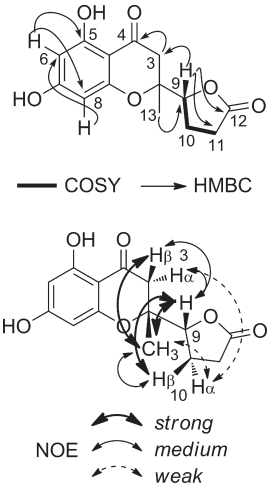

orientation of the lactone group with respect to the chromanone ring, as determined by the C-2/C-9 torsion. For (2*R*,9*R*)-**3**, the two most stable conformers (which differ in the orientation of 7-OH and account for 60% population) have the equatorial lactone ring almost perpendicular to the chromanone ring, and the CH_2-10 group is oriented toward the β face (see lowest-energy structure in Figure 3; other structures are shown in the Supporting Information). In this conformation, the H_2-10 and H_2-3 methylene protons are far from each other (at least 4.4 Å). This is also true for the next pair of conformers with an axial lactone group (17% population). Only for higher-energy pairs of conformers (10% and 7% populations) is H-3α closer to H-10α (2.8 and 3.4 Å, respectively). For (2*R*,9*S*)-**3**, on the contrary, the first five low-energy conformers (overall population of 73%) have H-3α and H-3β hydrogens close to H-10β and H-10α, respectively (2.3−3.2 and 2.5−3.6 Å; see structures in the Supporting Information). This conformational picture is compatible with NOESY experiments as far as the (2*R*,9*R*)-**3** diastereomer is concerned, but less for the (2*R*,9*S*) analogue. As a result, the relative configuration of microdiplodiasone has to be defined as (2*R**,9*R**)-**3**. We also calculated ^{13}C NMR magnetic shieldings[22] at the B3LYP-SCRF/6-311+G(d,p) level (with PCM in $CHCl_3$) on the two diastereomers, to be compared[23] with the experimental data recorded in $CDCl_3$. However, the two sets of calculated ^{13}C NMR chemical shifts (weighted average over the first five low-energy minima in both cases; see Supporting Information for details) were too similar to be used to discriminate between the two diastereomers, although they reproduced the experimental set (R^2 values around 0.988) very well.[23] It must be stressed that the related lachnone C has been assigned a (2*R**,9*S**) relative configuration on the basis of NOE results, which were, however, not substantiated by molecular modeling.[21] The comparison with blennolides, whose configuration at C-9 is again opposite that of compound **3**,[7] is less obvious because of the stressed structural differences.

To assign the absolute configuration of microdiplodiasone (**3**), the same ECD protocol described above for diversonol (**1**) was employed. The ECD spectrum of (+)-**3** in acetonitrile (Figure 4a) is consistent with those of other chromanone derivatives.[18] The first eight low-energy DFT structures (free energies within 1.4 kcal/mol and overall population 94% at

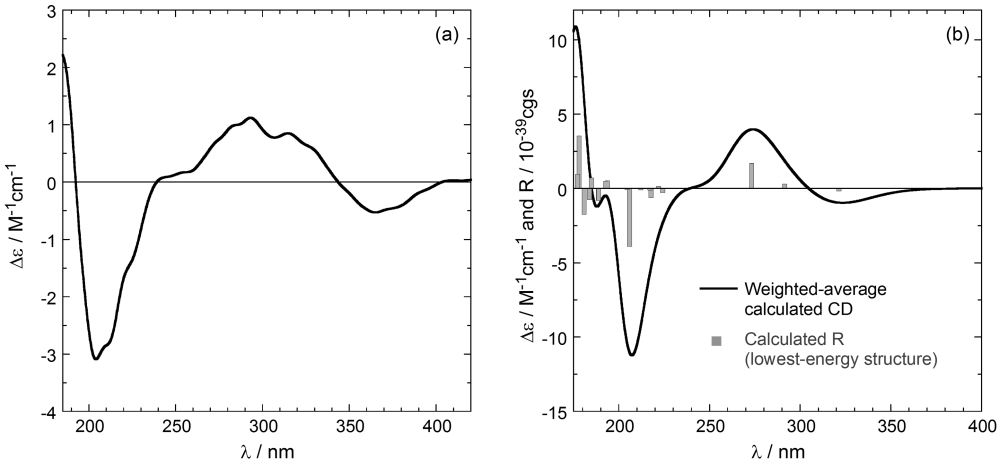

Figure 4. ECD spectra of (2*R*,9*R*)-(+)-microdiplodiasone (**3**). (a) Experimental spectrum in acetonitrile solution. (b) Weighted-average TDDFT-calculated spectrum at the B3LYP-SCRF/TZVP//B3LYP-SCRF/6-311+(d,p) level with PCM in MeOH. Vertical bars represent rotational strengths calculated for the lowest-energy conformer; Gaussian band shape with 0.3 eV width.

300 K) were employed for TDDFT calculations at the B3LYP/TZVP level.[24] As expected, the major determinant of the ECD spectrum is the helicity of the B ring: all structures with an axial 13-methyl group led to similar calculated spectra, and they were almost the mirror image of those calculated for structures with an equatorial 13-methyl group (see Supporting Information). The weighted-average calculated spectrum (Figure 4b) reproduced the experimental one over the whole spectral range very well. Thus, the absolute configuration of microdiplodiasone could be assigned as (2*R*,9*R*)-(+)-**3**. We also calculated the ECD spectra for the "wrong" (2*R*,9*S*) diastereomer, which, as anticipated, were similar to those of the (2*R*,9*R*) analogue. However, the weighted average spectrum for (2*R*,9*S*)-**3** (Supporting Information) lacked the low-energy negative ECD band found experimentally. In conclusion, we can confidently assign the (2*R*) absolute configuration, while the configuration at C-9 is less certain, though most probably it is (*R*), too.

Microdiplodiasolol (**4**) was isolated as optically active, yellow crystals with the molecular formula $C_{16}H_{16}O_7$, as deduced from HREIMS. The IR and UV spectra of **4** were reminiscent of those of **1**, showing functional absorption bands for hydroxy groups, carbonyl groups, and a typical 1,2,3,5-tetrasubstituted phenyl group. The presence of a hydrogen-bonded proton, resonating at δ_H 12.31 in the ^{1}H NMR spectrum, was observed similarly to **1**. Similarity of the A and B rings was also confirmed by comparison of the ^{13}C NMR spectra. However, two main differences were apparent in the spectrum of compound **4** with respect to ring C: first, the appearance of a low-field quaternary carbon at δ 173.6 instead of a methine carbon at C-5 (δ_C 66.3 and δ_H 4.32) as found in compound **1**; second, the two methylene signals in the ^{13}C NMR spectrum of compound **1** for C-6 (δ_C 24.9) and C-7 (22.7) were missing, and instead an α,β-unsaturated signal at δ_C 173.6 and a methine carbon at δ_C 99.8 appeared in the spectrum of **4**, together with a methine signal for H-6 (δ_H 5.32). Moreover, there was one methoxy group (δ_C 56.4 and δ_H 3.84) with HMBC correlation of its protons to C-5 (Scheme 4). Other HMBC correlations that assisted in the assignment of ring C were from H-6 to C-7, C-5, and C-5a; from H-8 to C-7, C-6, and C-8a; and from H-8 to the C-7 carbonyl (Scheme 4). Therefore, microdiplodiasolol (**4**) was determined as 1,8,8a-trihydroxy-5-methoxy-3,5a-dimethyl-5a,8a-dihydro-1*H*-xanthene-7,9-dione.

Scheme 4. Key HMBC Correlations for Compound 4

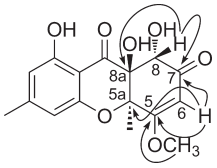

The ECD spectrum of (−)-**4** in MeOH (Figure 5a) is reminiscent of that of the chromanone family,[18] possibly with some interference from the enone chromophore. ECD bands at 210 and 280 nm have a sign opposite to the corresponding ones for (+)-**1**, which would imply a reversed configuration at the C-5a and C-8a stereogenic centers. Four DFT low-energy structures with a (5a*S*,8*S*,8a*S*) configuration were obtained differing in the orientation of the OH groups (Supporting Information). The weighted-average TDDFT-calculated ECD spectrum (Figure 5b) was again in good agreement with the experimental one (except in the ^{1}L$_b$ region above 330 nm) and allows assignment of the absolute configuration as (5a*S*,8*S*,8a*S*)-(−)-**4**. The average calculated optical rotation was −87.6, also in keeping with the experimental $[\alpha]_D$ −101 ± 5. It can be concluded, perhaps unexpectedly, that the two related compounds diversonol (**1**) and microdiplodiasolol (**4**) extracted from the same source have opposite absolute configuration at C-5a, C-8, and C-8a. The configuration at C-5 and C-5a of diversonol (**1**) corresponds to that found in blennolides A−C and in the dimeric compounds of the secalonic acid type.[7] The unexpected inverse (5a*S*,8*S*,8a*S*)-configuration of microdiplodiasolol (**4**) cannot be rationalized at the moment.

The molecular formula of microdiplactone (**5**) was assigned as $C_{11}H_{21}NO_2$ on the basis of HREIMS and ^{1}H and ^{13}C NMR spectroscopic data (see Experimental Section). IR absorption bands at 1735 cm^{-1} together with the corresponding carbon signals in the ^{13}C NMR spectrum at δ_C 173.5 (see Experimental Section) indicated the presence of a lactone group. The ^{13}C NMR spectrum of compound **5** displayed 11 carbon resonances, while the DEPT-135 experiment sorted these signals into two methyl, seven methylenes, one methine, and one quaternary carbon. The ^{1}H NMR spectrum in $CDCl_3$ exhibited one oxymethylene group

dx.doi.org/10.1021/np100730b |*J. Nat. Prod.* 2011, 74, 365–373

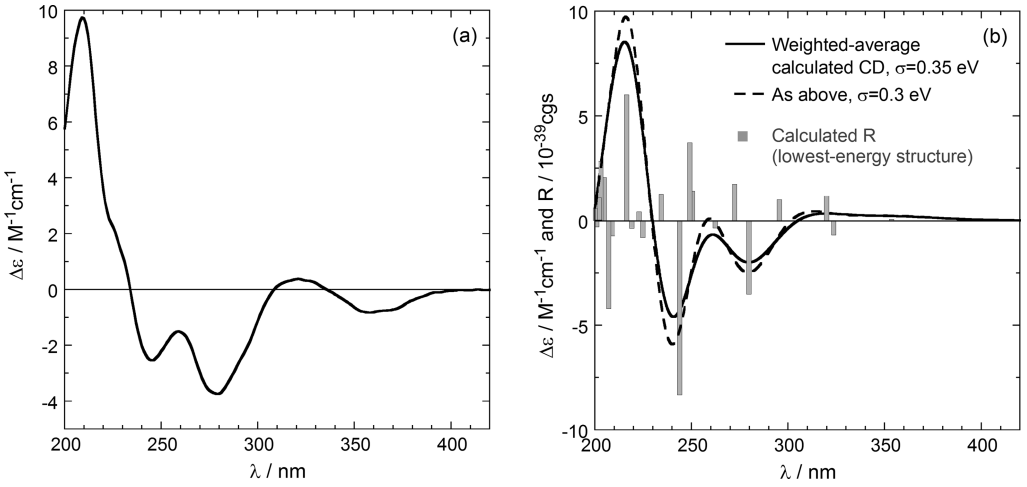

Figure 5. ECD spectra of (5a*S*,8*S*,8a*S*)-(−)-microdiplodiasolol (**4**). (a) Experimental spectrum in MeOH solution. (b) Weighted-average TDDFT-calculated spectrum at the B3LYP-SCRF/aug-TZVP//B3LYP-SCRF/6-311+(d,p) level with PCM in MeOH. Vertical bars represent rotational strengths calculated for the lowest-energy conformer; σ is the applied Gaussian band shape.

Scheme 5. COSY and Key HMBC Correlations for Compound 5

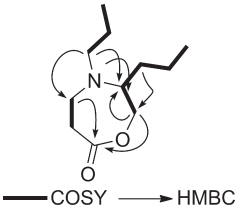

[δ_H 3.98 (dd, J = 14.5, 5.4 Hz, 2H, H-6)], two methylene signals [2.34 (t, J = 7.5 Hz, 2H, H-3), 2.95 (t, J = 7.5 Hz, 2H, H-2)], and two sets of signals for two propyl groups [δ_H 2.03 (m, 2H, H-1′), 1.35 (m, 2H, H-1″), 1.29 (m, 4H, H-2′, H-2″), 0.86 (t, J = 7.0 Hz, 6H, H-3′, H-3″)]. The correlations in the ^{1}H,^{1}H-COSY NMR spectrum were also consistent with two *n*-propyl units and one 1,4-oxazepin-7(2*H*)-one, and the interconnections between these units were determined through the relevant HMBC correlations (Scheme 5). The structure of **5** was determined by 2D NMR experiments, giving corresponding COSY and HMBC correlations (Scheme 5). The absolute configuration of microdiplactone (**5**) remains to be assigned.

Known compounds were identified by comparison with published data as emodin (**6**),[25] the two xanthones 1,8-dihydroxy-3-methoxy-6-methylxanthone (**7**)[26] and methyl 3,8-dihydroxy-6-methyl-9-oxo-9*H*-xanthene-1-carboxylate (**8**),[27] (−)-gynuraone (**9**),[28] and the steroid ergosterol (**10**)[29] (see Supporting Information).

Biological Activity. The metabolites **1**−**4** and **8**−**10** were tested for antibacterial activity in an MIC (minimum inhibitory concentration) test in liquid medium against *Legionella pneumophila* Corby, *Escherichia coli* K12, and *Bacillus megaterium,* and antifungal activity in an agar diffusion assay against the fungus *Microbotryum violaceum.* Except for **8**, the metabolites inhibited *L. pneumophila*; none of the metabolites inhibited *E. coli* or *B. megaterium.* Metabolites **2**, **4**, **8**, and **10** were antifungal against the fungal test organism *M. violaceum* (Table 1).

Table 1. Antibacterial (MIC test) and Antifungal Activities (agar diffusion assay) of Metabolites from *Microdiplodia* sp.[a]

	MIC test		agar diffusion assay
	Legionella pneumophila Corby		*Microbotryum violaceum* [radius of zone of inhibition in mm]
compound[b]	mg/mL	inhibition	50 μg
1	1.0	+	0
2	0.125−0.25	+	gi 7
3	1.0	+	0
4	1.0	+	6
8	1.0	−	6
9	1.0	+	n.t.
10	0.25−1.0	+	gi 7
penicillin	n.t.	n.t.	0
tetracycline	n.t.	n.t.	0
nystatin	n.t.	n.t.	20
actidione	n.t.	n.t.	50
kanamycin	0.0125−1.0	+	n.t.
acetone	0	−	0

[a] Legend: n.t. = not tested, + = inhibition, − = no inhibition, gi = some growth within the zone of inhibition. [b] The last 6 lines refer to control substances.

EXPERIMENTAL SECTION

General Experimental Procedures. For general methods and instrumentation see refs 30 and 31, and for microbiological methods and conditions of culture see ref 32. The melting points were determined on a Gallenkamp micromelting point apparatus and are uncorrected. Optical rotations were recorded on a Perkin-Elmer 241 polarimeter. ECD spectra were recorded on Jasco J-810 and J-715 spectropolarimeters using 0.01−0.1 cm cells.The NMR spectra were recorded on a Bruker-500 NMR Avance spectrometer (11.7 T) and a Varian INOVA 600 (14.1 T) spectrometer. Mass spectra were obtained on a MAT 8200

mass spectrometer (EI and HR-MS). Column chromatography was performed by using silica gel (Merck). Preparative TLC was performed on silica 20 × 20 cm TLC plates (Macherey and Nagel); compounds were detected by spraying with cerium−molybdenum spray reagent followed by heating.

Extraction and Isolation. The endophytic fungus *Microdiplodia* sp., internal strain No. 9907, was isolated from *Lycium intricatum* from Gomera, Spain, and cultivated on biomalt solid agar medium (12 L, 5% w/v) at room temperature for 28 days. The culture medium was then extracted with EtOAc to afford a residue (5.5 g) after removal of the solvent under reduced pressure. The extract was separated into three fractions by column chromatography (CC) on silica gel (200 g), with use of gradients of *n*-hexane/ethyl acetate (90:10, 50:50, 0:100). The more polar fractions (500 mg) were separated by silica gel column chromatography with elution with *n*-hexane/EtOAc (6:4) to give crude compound **1**, together with pure compound **2** (6.5 mg). The crude compound **1** was then recrystallized from EtOAc/*n*-hexane to give the pure natural product **1** (20 mg). Fraction B (400 mg) was separated by CC on silica gel (9 g) with *n*-hexane/EtOAc (8.5:1.5) to give three subfractions, B_{1-3}. Fraction B_3 (200 mg) was further separated by silica gel column chromatography and eluted with *n*-hexane/EtOAc (8:2) to give **3** (8 mg) and **4** (6 mg). Similarly compounds **5** (20 mg), **9** (6 mg), and **10** (15 mg) were isolated from fraction B_1 (400 mg), after elution with a mixture of *n*-hexane/EtOAc (8.7:1.3). Finally, repeated CC of fraction B_2 (300 mg), eluted with a mixture of *n*-hexane/EtOAc (8.5:1.5), gave **6** (16 mg), **7** (6 mg), and **8** (4 mg).

*Diversonol (**1**)*:. $[\alpha]^{29}_D$ +70 (*c* 0.33, MeOH); CD (MeCN, λ [nm] ($\Delta\varepsilon$), *c* 2.59 × 10^{-4}) 349 (−0.34), 321sh (0.62), 283 (1.14), 242sh (−0.25), 222sh (−2.99), 213 (−3.40); CD (KCl) λ (mdeg), 102 μg of **1** in 250 mg KCl, 352 (−6.59), 322sh (27.18), 296 (63.22), 244 (−3.35), 235 (11.25), 217sh (−71.98), 210 (−82.88); ^{1}H NMR (500 MHz, DMSO-d_6) δ 10.82 (s, 1 H, OH), 6.30 (br s, 1 H, H-2), 6.25 (br s, 1 H, H-4), 4.35 (m, *J* = 14.5 Hz, 1 H, H-5), 4.07 (m, *J* = 11.5 Hz, H-8), 2.05 (m, 1 H, H-6a), 2.00 (m, 1 H, H-7a), 1.84 (m, 1 H, H-6b), 1.70 (m, 1 H, H-6b), 1.46 (s, 3 H, H-11); ^{13}C NMR (125 MHz, $CDCl_3$+methanol-d_4) δ 194.7 (C-9), 162.0 (C-1), 159.0 (C-4a), 150.2 (C-3), 109.5 (C-2), 109.3 (C-4), 104.9 (C-9a), 81.6 (C-8a), 76.0 (C-5a), 73.9 (C-8), 66.8 (C-5), 24.4 (C-6), 21.4 (C-7), 22.3 (C-10), 19.8 (C-11); EIMS *m*/*z* (% rel int) 294.1 (21), 223 (13), 167 (100), 125 (12), 97 (14), 43(18), 18 (17); HREIMS *m*/*z* 294.1195 $[M]^+$ (calcd for $C_{15}H_{18}O_6$, 294.1103).

*Microdiplodiasol (**2**)*:. brown gum; $[\alpha]^{29}_D$ +6 (*c* 0.15, MeOH); ^{1}H NMR (500 MHz, $CDCl_3$+ methanol-d_4) δ 12.31 (s, 1 H, 1-OH), 11.30 (s, 1 H, 8a-OH), 6.51 (br s, 1 H, H-2), 6.62 (br s, 1 H, H-4), 5.43 (t, *J* = 5.5 Hz, 1 H, 10-OH), 4.59 (d, *J* = 5.5 Hz, 2 H, H-10), 4.22 (br d, *J* = 14.5 Hz, 1 H, H-5), 4.32 (br d, *J* = 11.5 Hz, H-8), 3.95 (s, 1 H, 5-OH), 3.75 (s, 1 H, 8-OH), 2.02 (m, 2 H, H-6), 1.84 (m, 2 H, H-7), 1.56 (s, 3 H-11); ^{13}C NMR (125 MHz, $CDCl_3$+methanol-d_4) δ 194.4 (C-9), 162.1 (C-1), 158.5 (C-4a), 153.2 (C-3), 105.9 (C-2), 105.7 (C-4), 104.6 (C-9a), 85.5 (C-8a), 75.6 (C-5a), 69.7(C-8), 66.9 (C-5), 63.5 (CH_2, C-10), 25.8 (C-6), 25.7 (C-7), 13.1 (C-11); IR (Nujol) ν_{max} 3555, 3410, 3355, 3245, 1659, 1633, 1572, 716 cm^{-1}; UV (MeOH) λ_{max} (log ε) 273 (4.09), 350 (3.50); EIMS *m*/*z* (% rel int) 310 (25), 223 (13), 167 (100), 125 (12), 97 (14), 43(18), 18 (17); HREIMS *m*/*z* 310.1052 $[M]^+$ (calcd for $C_{15}H_{18}O_7$, 310.1052).

*Microdiplodiasone (**3**)*:. yellow gum; $[\alpha]^{29}_D$ +14 (*c* 0.10, MeOH); CD (MeCN, λ [nm] ($\Delta\varepsilon$), *c* 7.6 × 10^{-3}) 365 (−0.52), 315 (0.85), 293 (1.12), 224sh (−1.43), 204 (−3.08); ^{1}H NMR (500 MHz, $CDCl_3$+methanol-d_4) δ 11.57 (s, 1 H, 5-OH), 11.45 (s, 1 H, 7-OH), 7.21 (br s, 1 H, H-8), 7.11 (br s, 1 H, H-6), 4.58 (t, *J* = 7.2 Hz, 1 H, H-9), 2.98 (d, *J* = 17.1 Hz, 1 H, H-3α), 2.61 (d, *J* = 17.1 Hz, 1 H, H-3β), 2.60 (m, 2 H, H-11), 2.32 (m, 2 H, H-10), 1.43 (s, 3H, H-13); ^{1}H NMR (600 MHz, acetonitrile-d_3) δ 7.02 (s, 1 H, H-8 or H-6), 6.99 (s, 1 H, H-6 or H-8), 4.64 (t, *J* = 7.5 Hz, 1 H, H-9), 3.08 (d, *J* = 17.1 Hz, 1 H, H-3α), 2.71 (d, *J* = 17.1 Hz, 1 H, H-3β), 2.55 (m, 2 H, H-11), 2.31 (m, 1 H, H-10β), 2.20 (m, 1 H, H-10α), 1.43 (s, 3H, H-13); ^{13}C NMR (125 MHz, $CDCl_3$+methanol-d_4) δ 196.6 (C-4), 176.6 (C-12), 166.0 (C-5), 161.2 (C-7), 158.6 (C-8a), 109.3 (C-4a), 110.6 (C-6), 108.9 (C-8), 82.7 (C-9), 81.1 (C-2), 42.8 (C-3), 28.1 (C-11), 22.2 (C-10), 18.8 (C-13); IR (neat) ν_{max} 3384, 1776, 1642 cm^{-1}; UV (MeOH) λ_{max} (log ε) 205 (3.64), 273 (3.01), 343 (2.93); EIMS *m*/*z* (% rel int) 278 (19), 221(100),181 (25), 152 (9), 85 (19), 57 (20), 43 (20), 18(42); HREIMS *m*/*z* 278.0949 $[M]^+$ (calcd for $C_{15}H_{16}O_6$, 278.0949).

*Microdiplodiasolol (**4**)*:. mp 236−238 °C; yellow crystals; $[\alpha]^{29}_D$ −101 (*c* 0.16, MeOH); CD (MeCN, λ [nm] ($\Delta\varepsilon$), *c* 2.84 × 10^{-4}) 358 (−0.96), 319 (0.26), 278 (−3.73), 245sh (−2.69), 226sh (1.43), 208 (8.53); ^{1}H NMR (500 MHz, $CDCl_3$+methanol-d_4) δ 12.31 (s, 1 H, 1-OH),11.30 (s, 1 H, 8a-OH), 6.37 (br s, 1 H, H-2), 6.45 (br s, 1 H, H-4), 5.32 (br s, 1 H, H-6), 5.18 (br s, 1 H, H-8), 3.84 (s, 3 H, OCH_3), 3.75 (s, 1 H, 8-OH), 2.25 (s, 3 H, CH_3-10), 1.56 (s, 3 H, CH_3 −11); ^{13}C NMR (125 MHz, $CDCl_3$+methanol-d_4) δ 193.1 (C-9), 192.4 (C-7), 173.6 (C-5), 162.2 (C-1), 157.1 (C-4a), 150.6 (C-3), 109.9 (C-2), 108.5 (C-4), 104.6 (C-9a), 99.8 (C-6), 84.2 (C-8a), 72.2 (C-5a), 69.7 (C-8), 56.4 (5-OCH_3), 22.1 (C-10), 13.1 (C-11); IR (Nujol) ν_{max} 3555, 3410, 3355, 3245, 1659, 1633, 1572 cm^{-1}; UV (MeOH) λ_{max} (log ε) 273 (4.09), 350 (3.50); EIMS *m*/*z* (% rel int) 320 (30), 207 (60), 151 (100), 139 (15), 86 (10), 43 (13), 18 (18); HREIMS *m*/*z* 320.0896 $[M]^+$ (calcd for $C_{16}H_{16}O_7$, 320.0896).

*Microdiplactone (**5**)*:. oil; ^{1}H NMR (500 MHz, $CDCl_3$) δ 3.98 (dd, *J* = 14.5, 5.4 Hz, 2H, H-6), 2.95 (t, *J* = 7.5 Hz, 2H, H-2), 2.34 (t, *J* = 7.5 Hz, 2H, H-3), 2.03 (m, 2H, H-1′), 1.57 (m, 1H, H-7), 1.35 (m, 2H, H-1″, 1.29 (m, 4H, H-2′, H-2″), 0.86 (t, *J* = 7.0 Hz, 6H, H-3′, H-3″); ^{13}C NMR (125 MHz, $CDCl_3$) δ 173.5 (C-4), 66.8 (C-6), 53.4 (C-7), 38.8 (C-5), 34.0 (C-2), 30.4 (C-1′), 28.9 (C-1″), 24.5 (C-2), 23.8 (C-2″), 22.9 (C-2′), 14.11 (C-3′), 10.9 (C-3″); IR (Nujol) ν_{max} 2939, 1735 cm^{-1}; HREIMS *m*/*z* 199.1568 $[M]^+$ (calcd for $C_{11}H_{21}NO_2$, 199.1572).

*Emodin (**6**), 1,8-Dihydroxy-3-methoxy-6-methylxanthone (**7**), Methyl 3,8-Dihydroxy-6-methyl-9-oxo-9H-xanthene-1-carboxylate (**8**), (−)-Gynuraone (**9**), and Ergosterol (**10**)*. For experimental data see Supporting Information.

*Crystal Structure Determination of **1** (ref 33)*. $C_{15}H_{18}O_6$, M_r = 294.3, colorless prismatic crystals (0.32 × 0.20 × 0.19 mm) orthorhombic, space group $P2_12_12_1$, *a* = 6.6836(3) Å, *b* = 10.0994(5) Å, *c* = 19.5108(9) Å, *V* = 1316.99(11) Å^3, *Z* = 4, ρ_{calc} = 1.484 g cm^{-3}, *F*(000) = 624, μ = 0.115 mm^{-1}. Data were collected at 120(2) K, Bruker SMART APEX CCDC diffractometer, Mo Kα radiation, λ = 0.71073 Å, θ_{max} = 27.9°, 12 395 measured reflections, of which 1822 were unique with $I > 2\sigma(I)$, R_{int} = 0.029. Structure solved by direct methods,[34] full-matrix least-squares refinement[34] with 1822 independent reflections based on F^2 and 195 parameters, all but H atoms refined anisotropically, H atoms from difference Fourier maps refined with riding model on idealized positions with $U = 1.5U_{iso}$(O and methyl-C) or $1.2U_{iso}$(C). Compound **1** crystallizes in the non-centrosymmetric space group $P2_12_12_1$; however, in the absence of significant anomalous scattering effects, the Flack parameter[35] is essentially meaningless. Accordingly, Friedel pairs were merged. Refinement converged at R1($I > 2\sigma(I)$) = 0.036, wR2(all data) = 0.100, *S* = 1.05, max(δ/σ) < 0.001, min./max. height in final ΔF map −0.21/0.40 e/Å^3. Figure 1 shows the molecular structure.

Assays for Biological Activity. For the agar diffusion assay, the compounds and control substances were dissolved in acetone at a concentration of 1 mg/mL. Fifty microliters of the solutions (50 μg) was pipetted onto a sterile filter disk (Schleicher & Schuell, 9 mm), which was placed onto MPY agar growth medium and subsequently sprayed with a suspension of the fungal test organism, *Microbotryum violaceum*.[36] Following incubation at 20 °C, commencing at the middle of the filter disk, the radius of the zone of inhibition was measured in millimeters.

The MIC assays were conducted in 200 μL well microtiter plates in liquid media. *Legionella pneumophila* Corby was tested in YEB medium (10 g ACES, 10 g yeast extract, 1000 mL Milli Q water, pH 6.9, to which

the following sterile filtrates are added: 0.4 g cysteine in 10 mL Milli-Q water, 0.25 g ferric pyrophosphate in 10 mL Milli-Q).

Computational Section. Molecular mechanics and preliminary DFT calculations were run with Spartan '08 (Wavefunction, Inc., Irvine, CA) with standard parameters and convergence criteria. DFT and TDDFT calculations were run with Gaussian '09,[37] with default grids and convergence criteria.

Conformational searches were run employing the "systematic" procedure implemented in Spartan '08, using MMFF (molecular Merck force field). All MMFF minima were reoptimized with DFT at the B3LYP/6-31G(d) level and then at the B3LYP/6-311+G(d,p) level using the integral equation formalism variant of the polarizable continuum model (IEF-PCM)[38] for the appropriate solvent with default parameters. Zero-point-corrected free energies were evaluated from frequency calculations at the same level of theory. TDDFT calculations were run using various combinations of the hybrid DFT functionals B3LYP, CAM-B3LYP, and BH&HLYP and the basis sets SVP, TZVP, and aug-TZVP,[39] including at least 24 excited states in all cases, and using IEF-PCM for MeOH or MeCN. The aug-TZVP set was constructed by augmenting TZVP with a (1s1p1d/1s1p) set of primitive functions taken from the most diffuse functions of aug-cc-pVDZ. All transitions computed with B3LYP/aug-TZVP (for compounds **1** and **4**) and B3LYP/TZVP (for compound **3**), and responsible for the ECD bands observed above 200 nm, had energies below the estimated ionization potentials. ECD spectra were generated using the program SpecDis[40] by applying a Gaussian band shape with 0.25−0.35 eV width, from dipole-length rotational strengths; the difference from dipole-velocity values was negligible (<10%) for most transitions.

Optical rotations at the sodium D line were obtained by dipole electric field polarizability calculations at the B3LYP/aug-TZVP level using IEF-PCM for MeOH. Magnetic shieldings σ were computed with the GIAO method at the B3LYP/6-311+G(d,p) level using IEF-PCM for $CHCl_3$ and converted into chemical shifts δ (in ppm) by the regression $\delta = 175.13 - 0.9683\sigma$, which is appropriate for the level of calculation.[23]

■ ASSOCIATED CONTENT

Supporting Information. DFT-optimized structures and calculated CD spectra for compounds **1**, **3**, and **4**; calculated ^{13}C NMR chemical shifts for compound **3**; ^{1}H and ^{13}C NMR spectra for compounds **1**−**5**; spectroscopic data for compounds **6**−**10** (PDF). This material is available free of charge via the Internet at http://pubs.acs.org.

■ AUTHOR INFORMATION

Corresponding Author
*E-mail: ripes@dcci.unipi.it (G.P.), k.krohn@upb.de (K.K.).

■ ACKNOWLEDGMENT

We wish to thank the Higher Education Commission Islamabad Pakistan, for a financial grant to two of us (I.N.S. and A.Z.), under the International Linkages of Pakistani Universities with foreign universities. T.K. thanks the Hungarian National Office for Research and Technology (NKTH, K-68429) and the János Bolyai Foundation.

■ DEDICATION

Dedicated to Prof. Koji Nakanishi of Columbia University for his pioneering work on bioactive natural products.

■ REFERENCES

(1) Schulz, B.; Boyle, C.; Draeger, S.; Rommert, A. K.; Krohn, K. *Mycol. Res.* **2002**, *48*, 996–1004.
(2) A total of 1464 hits were found for the unsubstituted xanthone skeleton in the Chapman and Hall Natural Products database, CRC Press, 2009.
(3) *The Biosynthesis of Mycotoxins. A Study in Secondary Metabolism*; Steyn, P. S., Ed.; Academic Press: New York, 1980.
(4) Peres, V.; Nagem, T. J. *Quim. Nova* **1997**, *20*, 388–397.
(5) Imperato, F. *Z. Naturforsch. B* **1990**, *45*, 1603–1604.
(6) (a) Huneck, S.; Yoshimura, I. *Identification of Lichen Substances*; Springer Verlag: Berlin, 1996. (b) Rezanka, T.; Sigler, K. *J. Nat. Prod.* **2007**, *70*, 1487–1491.
(7) Zhang, W.; Krohn, K.; Zia-Ullah; Flörke, U.; Pescitelli, G.; Di Bari, L.; Antus, S.; Kurtán, T.; Rheinheimer, J.; Draeger, S.; Schulz, B. *Chem.—Eur. J.* **2008**, *14*, 4913–4923.
(8) Wijeratne, E. M. K.; Turbyville, T. J.; Fritz, A.; Whitesell, L.; Gunatilaka, A. A. L. *Bioorg. Med. Chem.* **2006**, *14*, 7917–7923.
(9) Kawahara, N.; Sekita, S.; Satake, M.; Udagawa, S.; Kawai, K. *Chem. Pharm. Bull.* **1994**, *42*, 1720–1723.
(10) Tabata, N.; Tomoda, H.; Matsuzaki, K.; Omura, S. *J. Am. Chem. Soc.* **1992**, *114*, 8558–8564.
(11) Parish, C. A.; Smith, S. K.; Calati, K.; Zink, D.; Wilson, K.; Roemer, T.; Jiang, B.; Xu, D.; Bills, G.; Platas, G.; Peláez, F.; Díez, M. T.; Tsou, N.; McKeown, A. E.; Ball, R. G.; Powles, M. A.; Yeung, L.; Liberator, P.; Harris, G. *J. Am. Chem. Soc.* **2008**, *130*, 7060–7066.
(12) Corrado, M.; Rodrigues, K. F. *J. Basic Microbiol.* **2004**, *44*, 157–160.
(13) Turner, W. B. *J. Chem. Soc., Perkin Trans. 1* **1978**, 1621 (in this publication it is not clear whether the isolated compound was racemic or enantiopure).
(14) Holker, J. S.; O'Brien, E.; Simpson, T. J. *J. Chem. Soc., Perkin Trans. 1* **1983**, 1365–1368.
(15) (a) Nicolaou, K. C.; Li, A. *Angew. Chem., Int. Ed.* **2008**, *47*, 6579–6582. (b) Nising, C. F.; Ohnemüller, U. K.; Bräse, S. *Angew. Chem., Int. Ed.* **2006**, *45*, 307–309.
(16) (a) Autschbach, J. *Chirality* **2009**, *21*, E116–E152. (b) Di Bari, L.; Pescitelli, G. In *Computational Spectroscopy—Methods, Experiments and Applications*; Grunenberg, J., Ed.; Wiley-VCH: Weinheim, 2010; pp 241−277.
(17) Pescitelli, G.; Kurtán, T.; Flörke, U.; Krohn, K. *Chirality* **2009**, *21*, E181–E201.
(18) Dai, J.; Krohn, K.; Flörke, U.; Draeger, S.; Schulz, B.; Kiss-Szikszai, A.; Antus, S.; Kurtán, T.; van Ree, T. *Eur. J. Org. Chem.* **2006**, 3498–3506.
(19) (a) Pescitelli, G.; Di Bari, L.; Caporusso, A. M.; Salvadori, P. *Chirality* **2008**, *20*, 393–399. (b) Mazzini, F.; Pescitelli, G.; Di Bari, L.; Netscher, T.; Salvadori, P. *Chirality* **2009**, *21*, 35–43.
(20) (a) Crawford, T. D.; Tam, M. C.; Abrams, M. L. *J. Phys. Chem. A* **2007**, *111*, 12057–12068. (b) Autschbach, J. *Comput. Lett.* **2007**, *3*, 131–150. (c) Stephens, P. J.; McCann, D. M.; Cheeseman, J. R.; Frisch, M. J. *Chirality* **2005**, *17*, S52–S64.
(21) Rukachaisirikul, V.; Chantaruk, S.; Pongcharoen, W.; Isaka, M.; Lapanun, S. *J. Nat. Prod.* **2006**, *69*, 980–982.
(22) Bifulco, G.; Dambruoso, P.; Gomez-Paloma, L.; Riccio, R. *Chem. Rev.* **2007**, *107*, 3744–3779.
(23) Van Eikema Hommes, N. J. R.; Clark, T. *J. Mol. Model* **2005**, *11*, 175–185.
(24) On a few lowest-energy conformers we verified that inclusion of diffuse functions (use of aug-TZVP instead of TZVP) did not alter significantly the shape of calculated CD spectra.
(25) Zhou, X.; Song, B.; Jin, J.; Hu, D.; Diao, C.; Xu, G.; Zhou, Z.; Song, Y. *Bioorg. Med. Chem. Lett.* **2006**, *16*, 563–568.
(26) Sob, S. V. T.; Wabo, H. K. *Tetrahedron* **2008**, *64*, 7999–8002.
(27) Hamasaki, T.; Kimura, Y. *Agric. Biol. Chem.* **1983**, *47*, 163–165.
(28) Lin, W. Y.; Kuo, Y. H.; Chang, Y. L.; Teng, C. M.; Wang, E. C.; Ishikawa, T.; Chen, I. S. *Planta Med.* **2003**, *69*, 757–764.
(29) Goulston, G.; Mercer, E. I.; Goad, L. J. *Phytochemistry* **1975**, *14*, 457–462.

(30) Dai, J.; Krohn, K.; Gehle, G.; Kock, I.; Flörke, U.; Aust, H. J.; Draeger, S.; Schulz, B.; Rheinheimer, J. *Eur. J. Org. Chem.* **2005**, 4009–4016.

(31) Krohn, K.; Flörke, U.; Rao, M. S.; Steingröver, K.; Aust, H.-J.; Draeger, S.; Schulz, B. *Nat. Prod. Lett.* **2001**, *15*, 353–361.

(32) Schulz, B.; Sucker, J.; Aust, H.-J.; Krohn, K.; Ludewig, K.; Jones, P. G.; Doering, D. *Mycol. Res.* **1995**, *99*, 1007–1015.

(33) Full crystallographic data (excluding structure factors) for **1** have been deposited with the Cambridge Crystallographic Data Centre as supplementary publication no. CCDC-795740. Copies of the data can be obtained free of charge on application to CCDC, 12 Union Road, Cambridge CB2 1EZ, UK (fax: (+44)1223-336-033; e-mail: deposit@ccdc.cam.ac.uk).

(34) Bruker. *SMART* (Version 5.62), *SAINT* (Version 6.02); Bruker AXS Inc.: Madison, WI, USA, 2002.

(35) Flack, H. D. *Acta Crystallogr.* **1983**, *A39*, 876–881.

(36) Höller, U.; Wright, A. D.; Matthée, G. F.; König, G. M.; Draeger, S.; Aust, H.-J.; Schulz, B. *Mycol. Res.* **2000**, *104*, 1354–1365.

(37) Frisch, M. J.; et al. *Gaussian 09*, Revision A.02; Gaussian, Inc.: Wallingford, CT, 2009 (complete reference given in the Supporting Information).

(38) *Continuum Solvation Models in Chemical Physics: From Theory to Applications*; Tomasi, J.; Mennucci, B.; Cammi, R., Eds.; Wiley: Chichester, 2007.

(39) See Gaussian '09 documentation at www.gaussian.com/g_tech/g_ur/g09help.htm for references on DFT functionals and basis sets.

(40) Bruhn, T.; Hemberger, Y.; Schaumlöffel, A.; Bringmann, G. *SpecDis* version 1.50; University of Wuerzburg: Germany, 2010.